JMEPEG (2011) 20:114–119
DOI: 10.1007/s11665-010-9653-x

1059-9495/$19.00

An Alternate Approach to Accelerated Spheroidization in Steel by Cyclic Annealing

Atanu Saha, Dipak Kumar Mondal, and Joydeep Maity

(Submitted September 30, 2009; in revised form February 6, 2010)

In this work an annealed 0.6 wt.% carbon steel was subjected to cyclic heat treatment process that consisted of repeated short-duration (6 min) holding at 810 °C (above Ac_3 temperature) followed by cooling in a flowing air medium (flow rate: 6 m^3/h). After 8 cycles (about 1 h and 20 min), the microstructure mostly contains spheroidized cementite and ferrite along with trace amount (3%) of pearlite. In addition to the diffusion within lamella, the disintegration of lamellae through dissolution of cementite at preferred sites of lamellar faults during short-duration holding above Ac_3 temperature, and the generation of defects (lamellar faults) during non-equilibrium cooling in a flowing air medium are the main reasons of accelerated spheroidization.

Keywords accelerated spheroidization, carbon steel, cementite dissolution, cyclic heat treatment, lamellar faults

1. Introduction

The conventional spheroidization process of steel consists of a subcritical annealing treatment that takes a long time. In an annealed Fe-0.79 wt.% C alloy, the spheroidization remains incomplete even after 100 h of holding at 700 °C (Ref 1). In 0.72%C steel with fine pearlitic structure, isothermal annealing at 680 °C requires 72 h of holding for nearly 100% spheroidization, whereas with coarse pearlitic structure, 50 h of holding only causes 50% spheroidization (Ref 2). Therefore, it has been a challenge for steel industry to accelerate the spheroidization of pearlitic structure. Since the isothermal annealing slightly below Ac_1 temperature is a long process for spheroidization, several other processes have been developed such as (a) thermal cycling near Ac_1 temperature, (b) isothermal annealing with the aid of prior cold work, (c) hot deformation before, during, or after the transformation of austenite to pearlite, and (d) decomposition of supercooled austenite at a temperature slightly below Ac_1 (Ref 3). The thermal cycling (swinging annealing) of ±5 °C around Ac_1 temperature facilitates the dissolution of cementite lamellae when temperature is raised above Ac_1. At subsequent cooling below Ac_1 this dissolution process is interrupted and the broken cementite particles coagulate more easily and quickly (Ref 4). Baranova and Sukhomlin (Ref 5) observed that the prior cold working generates defects in the atomic crystal structure of both ferrite and cementite that affects mechanism and kinetics of pearlite spheroidization. Under the influence of previous cold work, during subcritical annealing of steel, the process of cementite separation into pieces is made easier. During subcritical annealing, the cementite in worked steel is found to disintegrate along slip bands, grain, or subgrain boundaries of ferrite. Zhang et al. (Ref 6) applied a uniaxial compression at pearlitic transformation incubation temperature in order to accelerate spheroidization in steel. The microstructural evolution process of the steel during deformation included pearlitic transformation, cementite spheroidization, and ferrite recrystallization. Two microprocesses of cementite spheroidization were observed. The first one was the dissolution and subsequent breakdown of cementite lamellae; whereas the other involved precipitation of finer cementite particles in the ferrite matrix during recrystallization of ferrite. In contrast, Zhu and Zheng (Ref 7) studied a direct spheroidization process during hot rolling of hypereutectoid GCr15 steel. The direct spheroidization is promoted by a combination of low deformation temperature and slow cooling rate that happens to augment the divorced eutectoid transformation reaction. Under such conditions, during phase transformation carbide particles are likely to grow independently on the pre-existing carbide 'nuclei' and result in a poor carbon area to form ferrite. This generates a final microstructure consisting of a ferrite matrix and spheroidized carbide particles. Another method of accelerated spheroidization (known as 'complete thermal cycling process') involves austenitizing followed by rapid quenching to a temperature slightly above the martensite-start transformation temperature (M_s), finally up-quenching to a temperature slightly below the Ac_1 temperature for isothermal annealing. The supercooled austenite possesses large dislocation density and during subcritical annealing just below the Ac_1 temperature, these dislocations aid the nucleation of cementite particles. This causes a rapid spheroidization through the abnormal decomposition of austenite (Ref 3).

Cyclic heat treatments are found to accelerate several solid state metallurgical processes. Sista et al. (Ref 8) applied a cyclic austempering technique to accelerate bainitic transformation in 1080 steel. Sahay et al. (Ref 9) found an accelerated grain growth behavior in a cold rolled AlK-grade steel (0.05%C, 0.05%Al, and 45 ppm N) subjected to cyclic annealing

Atanu Saha, NDT and Metallurgy Group, Central Mechanical Engineering Research Institute, Durgapur 713209 West Bengal, India; and **Dipak Kumar Mondal** and **Joydeep Maity**, Department of Metallurgical and Materials Engineering, National Institute of Technology Durgapur, Durgapur 713209 West Bengal, India. Contact e-mail: joydeep_maity@yahoo.co.in.

treatment. The landmark research work carried out by Verhoeven (Ref 10) and Verhoeven and Gibson (Ref 11) has established that the austenite containing fine particles of carbides may undergo divorced eutectoid transformation reaction that produces a spheroidized structure in steel for austenitization at temperatures of 830 °C and below. The present investigation applies a cyclic heat treatment process that consists of repeated short-duration holding at 810 °C (above the Ac_3 temperature to generate a microstructure consisting of austenite plus cementite) followed by cooling in a flowing air medium (flow rate: 6 m^3/h) in order to accelerate spheroidization process in a 0.6 wt.%C steel.

2. Experimental Procedure

2.1 Cyclic Heat Treatment

As-received material was an annealed 0.6%C steel. Chemical composition of the steel as analyzed by an optical emission spectrometer (WAS, FMSN: 01G 00 26) is given in Table 1. Annealed steel bars of dimension 75 by 13 by 6 mm were subjected to cyclic heat treatment for different number of cycles, viz. 1-cycle, 3-cycle, 5-cycle, and 8-cycle. Each cycle consists of inserting the specimen in an electric resistance furnace at 810 °C (above Ac_3 temperature, 760 °C) and holding for 6 min, followed by cooling in a flowing air medium (forced air cooling) to the room temperature. In each cycle, the air flow rate was maintained at 6 m^3/h (using a blower) with a total cooling time of 4 min. In order to study the extent of cementite dissolution, one as-received specimen of similar dimension was heated to 810 °C, held for 6 min and quenched in ice-brine solution.

2.2 Optical Metallography

All specimens were sectioned to small pieces and polished with successive grades of emery papers up to 1000 grit size followed by cloth polishing with 1 μm diamond paste. Thereafter, these specimens were etched by 2% NITAL and examined under metallurgical microscope (Leica, Reichert, Polyvar2). Percentage of different micro-constituents present on two-dimensional specimen surface was determined using the point count method at a magnification 800× in a unit consisting of optical microscope (Reichert, Austria, Nr.311586) equipped with graduated eye piece and point counter (James Swift & Sons Ltd., Basingstokf, England).

Table 1 Chemical composition of as-received steel (wt.%)

C	Si	Mn	P	S	Cr	Cu	Ni	Al	Fe
0.580	0.280	0.540	0.022	0.017	0.080	0.035	0.030	0.006	Balance

2.3 Scanning Electron Microscopy

In order to investigate further details, polished and etched specimens were examined in a Scanning Electron Microscope (Hitachi, S-3000N) under secondary electron image mode. The size of the cementite spheroids were measured from SEM-images at high magnification. According to published literature (Ref 3), the spheroidized cementite particles in steel are considered to be the 'oblate spheroids' with aspect ratio represented by the ratio of the minor axis to the major axis. In the present study, each spheroid is considered as an approximated ellipse in the two-dimensional SEM image with aspect ratio lying in a range of 0.7-1.0. The cementite particles with aspect ratio less than 0.7 are not considered as 'spheroids.'

3. Results and Discussion

The microstructures of the specimen held at 810 °C for 6 min followed by quenching in ice-brine solution are shown in Fig. 1(a)-(c). The presence of partially dissolved cementite lamellae (Fig. 1a-b) indicates that during holding at 810 °C (above Ac_3 temperature) for 6 min, the dissolution of cementite lamellae in pearlitic region remains incomplete. After ice-brine quenching the matrix region in proximity with incompletely dissolved cementite exhibits the presence of high carbon martensite (Fig. 1b); whereas, the region away shows the presence of low carbon martensite (Fig. 1c). This indicates the inhomogeneity in austenite at 810 °C. Before ice-brine quenching, the austenite matrix around partially dissolved cementite lamellae was carbon-enriched and the austenite regions away (mainly prior proeutectoid ferrite regions) were carbon-devoid.

The optical micrographs of the as-received annealed specimen and the specimens subjected to heat treatment for different number of cycles are presented in Fig. 2(a)-(e). The result of point count analysis is shown in Table 2. According to point count analysis, the as-received steel, in annealed condition, contains 72% pearlite and 28% proeutectoid ferrite. In the first cycle, during holding above Ac_3 temperature, the proeutectoid

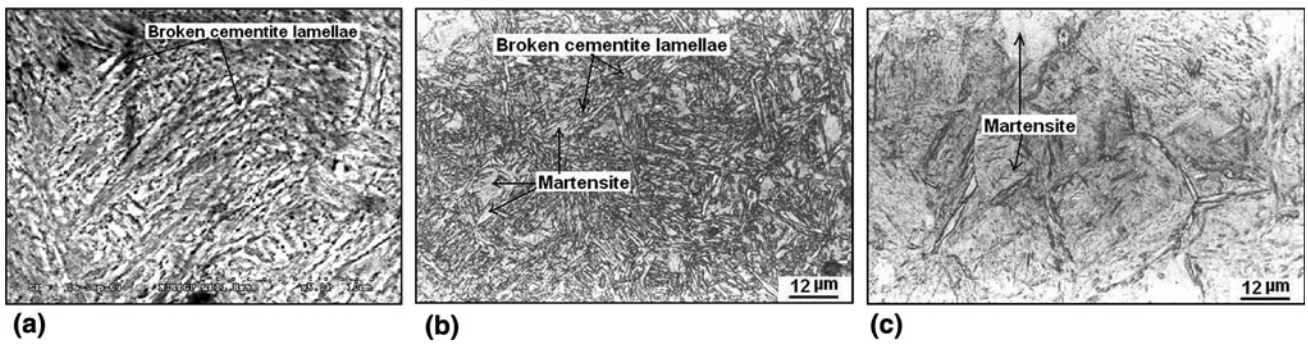

Fig. 1 Microstructures of the specimen quenched from 810 °C after holding for 6 min: (a) SEM secondary electron image, (b) optical image: partially dissolved cementite region, and (c) optical image: prior proeutectoid ferrite region

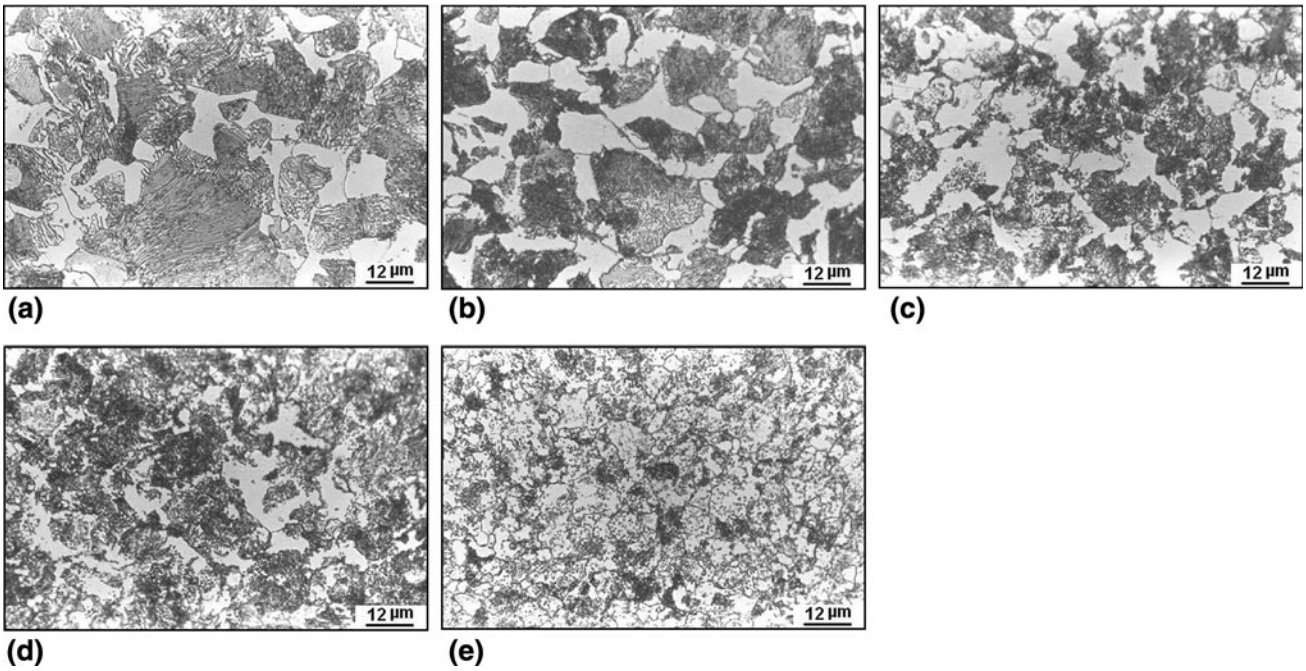

Fig. 2 The optical micrographs of the as-received annealed specimen and the specimens subjected to heat treatment for different number of cycles: (a) as-received, (b) 1-cycle, (c) 3-cycle, (d) 5-cycle, and (e) 8-cycle

Table 2 Result of point count analysis

No. of heat treatment cycles	% Ferrite	% Pearlite	% Cementite spheroids
0	28	72	Negligible
1	39	61	Negligible
3	44	46	10
5	46	39	15
8	61	3	36

ferrite zone is expected to transform into austenite quite rapidly. Whereas, in the pearlitic regions, austenitization starts at ferrite-cementite interface. The ferrite at ferrite-cementite interface rapidly transforms to austenite. The ferrite-to-austenite transformation is a diffusionless massive polymorphic transformation that occurs extremely fast (Ref 12). Thereafter, the cementite lattice breaks down and it dissolves in austenite at the austenite-cementite interface as iron atoms join the austenite lattice and carbon atoms diffuse to the octahedral interstices of austenite. Further, carbon atoms diffuse within austenite from the austenite-cementite interface to the ferrite-cementite interface owing to concentration gradient. The rate of migration of the austenite-ferrite interface is much faster than the austenite-cementite interface as it does not involve any diffusion (Ref 12, 13). Therefore, the dissolution of cementite in austenite is a slow process and in the present investigation during holding of 0.6 wt.%C steel at 810 °C for 6 min, the dissolution of cementite remains incomplete. It is expected that only in a small region around cementite lamellae the austenite is enriched with carbon and in the remaining part of matrix the austenite is devoid of carbon due to insufficient diffusion time available. At 810 °C, in the most part of austenite-matrix the carbon content remains much less than 0.6 wt.%. During forced air cooling the carbon-depleted regions (major portion) transforms mostly into ferrite and carbon enriched region (relatively small portion) around partially dissolved fragmented cementite converts into fine pearlite. This reduces the overall proportion of pearlite and increases the proportion of ferrite in the microstructure after single heat treatment cycle as indicated in Table 2. The SEM secondary electron image (Fig. 3a) exhibits broken cementite lamellae surrounded by fine pearlitic region in the steel heat treated for single cycle. The fragmented cementite lamellae appear in the form of long ribbons, rods, and sometimes as relatively thicker irregular shapes as shown in Fig. 3(a)-(c). While in most of the places fragmented cementite lamellae appear as ribbons or rods (Fig. 3a-b), at few places thick irregular shapes are found (Fig. 3c). The fragmented cementite lamellae are developed through partial dissolution of cementite at 810 °C. The surrounding regions of fine pearlite are originated from the carbon enriched austenite regions during forced air cooling. In Fig. 3(a), the fine pearlitic region is found at the junction between two pearlite colonies. Among different pearlite colonies the most probable location for the initiation of austenitization is the junction (Ref 12). Therefore, the cementite dissolution would be more complete at the junction forming a carbon enriched austenitic region at 810 °C, which upon forced air cooling converts into fine pearlite.

A real pearlitic lamellar structure is never perfect. A variety of lamellar faults such as kinks, striations, holes, fissures, and terminations always occur (Ref 1). The fragmentation of cementite lamellae into ribbon or rod shape mainly occurs through preferential dissolution of cementite at these sites of higher chemical potential during holding at 810 °C. The thickening of fragmented rod or ribbon (as indicated by thicker and irregular shape, Fig. 3c) is possible through diffusion of atoms from a lamellar fault site to adjacent flat surface of a cementite lamella. The lamellar fault sites in cementite lamellae are always the sites of higher chemical potential as compared to either the adjacent austenite or the adjacent flat surface of same

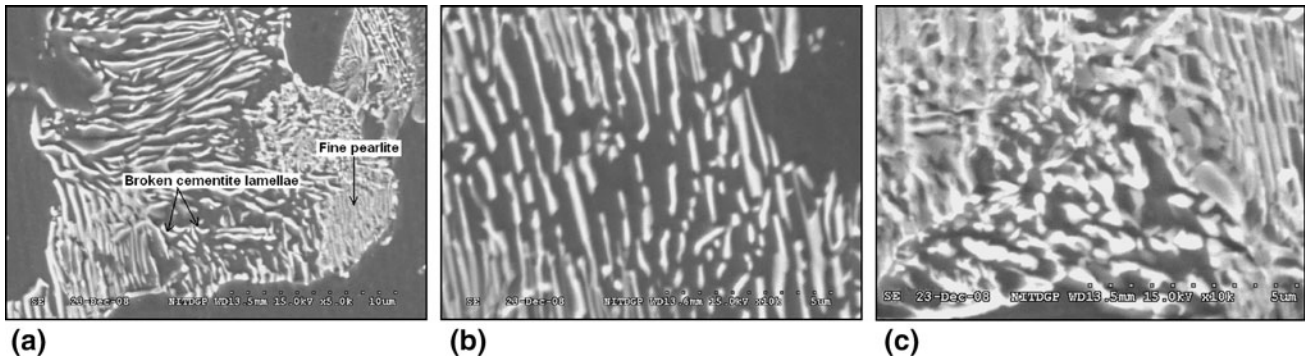

Fig. 3 SEM secondary electron images of the specimen subjected to single heat treatment cycle: (a) broken cementite (rod and ribbon shaped) and fine pearlite, (b) broken cementite (rod shaped) at higher magnification, and (c) broken cementite (thick irregular shaped) at higher magnification

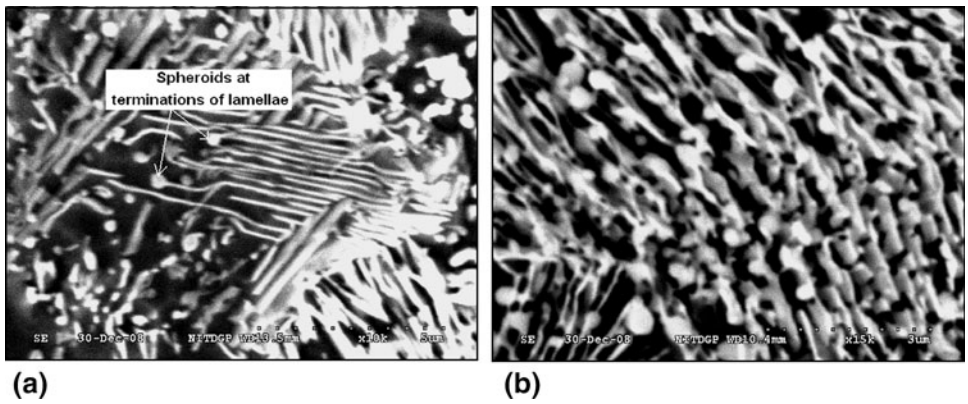

Fig. 4 SEM secondary electron images of the specimen subjected to three heat treatment cycles: (a) formation of spheroids at the terminations of lamellae and (b) formation of spheroids along the axis of lamellae

cementite lamella. The cementite lamellae-breakdown into rods or ribbons mainly occurs through the diffusion of atoms from the preferred sites of lamellar fault to the adjacent austenite. Such diffusional process is conventionally known as 'cementite dissolution' during the process of austenitization. On the other hand, the diffusion of atoms from the lamellar fault sites to the adjacent flat surfaces of a cementite lamella causes thickening of lamella. This diffusional process may be termed as 'diffusion within lamella.' This process may also have secondary effect on the fragmentation of a cementite lamella through the removal of atoms from fault regions. In the first cycle, thickening is observed only at few places and it appears not to be a major phenomenon at this stage. It is important to note that the main mechanism of conventional subcritical isothermal spheroidization is the atomic diffusion from highly curved lamellar fault sites to the neighboring flat interfaces as explained by 'fault migration theory' (Ref 1). Therefore, in the present study the lamellar breakdown is augmented by another high temperature diffusional process, i.e., the diffusion of atoms from lamellar fault sites to the adjacent austenite during austenitization. After first cycle, no spheroidized cementite particle (represented by the aspect ratio between 0.7 and 1.0) is observed and mainly the breakdown of cementite lamellae occurs. The breakdown of lamellar cementite into rod or ribbon shape is considered to be the first step of spheroidization process (Ref 1).

During second cycle, the finer pearlite surrounding the fragmented cementite lamellae is expected to undergo faster austenitization and rapid breakdown of lamellae. During first cycle, the nonequilibrium forced air cooling generates extremely fine pearlitic structure with expected more number of lamellar fault sites. This would make both the diffusional processes ('cementite dissolution' and 'diffusion within lamella') faster during second cycle. Therefore, cementite lamellae are expected to break into more number of smaller pieces during second cycle while holding at 810 °C for 6 min. This along with simultaneous thickening of lamellae results in the progress of spheroidization. Also, the fragmented cementite lamellae of previous cycle undergo spheroidization through diffusional processes. Again, due to partial dissolution of cementite, the overall carbon content of austenite decreases and upon forced air cooling more amount of ferrite is expected in the microstructure. Also, when a lamellar cementite converts into cementite spheroids, the pearlitic ferrite joins the matrix ferrite (proeutectoid ferrite). The process repeats in each of subsequent heat treatment cycles. Accordingly, with increasing number of cycles the relative proportion of pearlite decreases; whereas, the proportion of ferrite and cementite spheroids increases. This is in agreement with the results obtained by point count analysis (Table 2).

At higher magnification, SEM secondary electron image exhibits the generation of cementite spheroids at terminations of lamellae (Fig. 4a) as well as along the axis of lamellae (Fig. 4b) in the specimen subjected to three heat treatment cycles. This indicates the existence of lamellar faults (sites of

higher chemical potential) not only at the terminations of lamellae but also along the axis of lamellae. Several spheroids are found to be adhered to the lamellae and isolated spheroids are relatively less. For still higher number of heat treatment cycles (5-cycle) the spheroids tend to grow in size, their adherence to the lamellae is relatively less and their presence is more isolated (Fig. 5a-b). It is important to note that in case of higher heat treatment cycles, during holding at 810 °C for 6 min, austenitization is mainly restricted to the remaining pearlitic regions. Only at these locations the lamellar breakdown by partial cementite dissolution persists. On the other hand, austenitization would be sluggish in the regions containing isolated cementite spheroids. It is known that the kinetics of cementite dissolution is slow for spheroidized microstructure (Ref 12, 13). Therefore, dissolution of these spheroids is expected to be sluggish and during holding at higher temperature (810 °C) these isolated spheroids are expected to grow in size by the well known diffusional process, 'Ostwald ripening.' The measured size of isolated spheroids from SEM micrographs is presented in Table 3. Average size of isolated spheroids increases with increasing cycles of heat treatment. This indicates the growth of spheroids by Ostwald ripening. The reports on conventional subcritical isothermal spheroidization process have also mentioned Ostwald ripening as the process of spheroid growth (Ref 1). With increasing cycles of heat treatment the percent cementite spheroids in the microstructure (Table 2) as well as the spheroid size (Table 3) increases. This indicates that generation of spheroids and coagulation of spheroids (Ostwald ripening) proceed simultaneously.

Table 3 Size of isolated cementite spheroids

Number of heat treatment cycles	Size of spheroids, μm (Mean ± standard deviation)
1	No spheroid
3	0.39 ± 0.05
5	0.49 ± 0.14
8	0.53 ± 0.15

Finally, after 8 cycles of heat treatment the amount of lamellar pearlite in microstructure is reduced to only 3% (Table 2). The microstructure mainly contains spheroidized cementite and ferrite as shown in Fig. 6(a)-(b). Several isolated cementite spheroids with an average size of 0.53 ± 0.15 μm is visible. It is important to note that the total time required in execution of eight heat treatment cycles is about 1 h 20 min. The conventional subcritical spheroidization requires much longer time (about 100 h). Therefore, the present cyclic heat treatment process can be considered as an alternate route of accelerated spheroidization. The rapid spheroidization in the

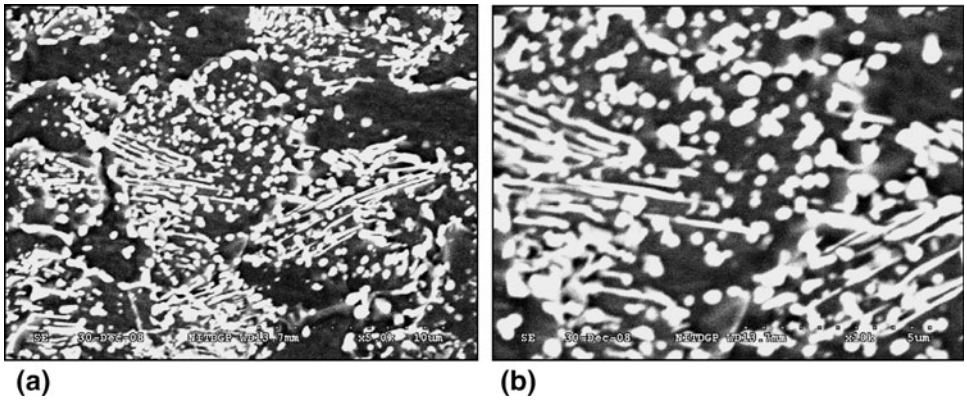

Fig. 5 SEM secondary electron images of the specimen subjected to five heat treatment cycles: (a) at lower magnification and (b) at higher magnification

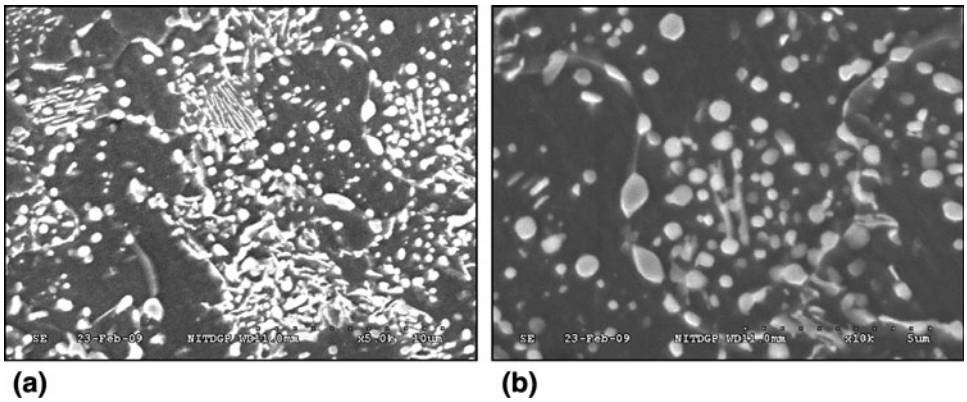

Fig. 6 SEM secondary electron images of the specimen subjected to eight heat treatment cycles: (a) at lower magnification and (b) at higher magnification

present investigation is mainly attributed to three major factors. Firstly, the process temperature is very high (above Ac_3) that makes all diffusional processes faster. Secondly, the incomplete cementite dissolution process augments spheroidization, which is absent in conventional subcritical spheroidization process. Thirdly, in each cycle, the nonequilibrium forced air cooling generates more lamellar faults that act as potential sites for the diffusion-assisted spheroidization process.

4. Conclusion

(i) The cyclic heat treatment consisting of repeated short-duration holding at 810 °C (above Ac_3) followed by cooling in a flowing air medium accelerates the spheroidization process in 0.6 wt.% carbon steel.

(ii) The fragmentation of lamellae is augmented by the dissolution of cementite through atomic diffusion from preferred sites of 'lamellar fault' (kinks, striations, holes, fissures, and terminations) in cementite to the adjacent austenite during short-duration holding above Ac_3 temperature. The diffusion of atoms from lamellar fault sites to the adjacent flat surface is mainly responsible for the thickening of lamellae and may also have secondary effect on lamellar fragmentation. The nonequilibrium air cooling is likely to generate more lamellar fault regions that act as the potential sites for spheroidization.

(iii) The first heat treatment cycle mainly causes the fragmentation of cementite lamellae into rod or ribbon shape. With three heat treatment cycles considerable presence (10%) of cementite spheroids (aspect ratio between 0.7 and 1.0) is observed. The generation of more spheroids and coagulation of spheroids (Ostwald ripening) proceed simultaneously with increasing cycles of heat treatment.

(iv) After eight heat treatment cycles the microstructure mostly contains spheroidized cementite particles in ferrite matrix along with trace amount (3%) of pearlite.

References

1. Y.L. Tian and R.W. Kraft, Mechanism of Pearlite Spheroidization, *Metall. Trans. A*, 1987, **18A**, p 1403–1414
2. D.K. Mondal and R.M. Dey, Effect of Structures on the Response to Spheroidization in a Eutectoid Plain Carbon Steel, *Trans. IIM*, 1984, **37**, p 351–356
3. C.C. Chou, P.W. Kao, and G.H. Cheng, Accelerated Spheroidization of Hypoeutectoid Steel by the Decomposition of Supercooled Austenite, *J. Mater. Sci.*, 1986, **21**, p 3339–3344
4. B. Liscic, Steel Heat Treatment, *Steel Heat Treatment Hand Book*, G.E. Totten and M.A.H. Howes, Ed., Marcel Dekker, New York, USA, 1997, p 596
5. V.A. Baranova and G.D. Sukhomlin, Spheroidization of Cementite in Steel, *Metallovedenie i Termicheskaya rabotka Metallov*, 1981, **11**, p 51–55
6. H. Zhang, B. Bai, and H. Fang, Effect of Prestrain on the Superplastic Deformation Behavior of Low-Alloy High-Carbon Steel, *Acta Metall. Sinica*, 2009, **45**, p 1106–1110
7. G. Zhu and G. Zheng, Directly Spheroidizing During Hot Deformation in GCr15 Steels, *Front. Mater. Sci. China*, 2008, **2**, p 72–75
8. V. Sista, P. Nash, and S.S. Sahay, Accelerated Bainitic Transformation During Cyclic Austempering, *J. Mater. Sci.*, 2007, **42**, p 9112–9115
9. S.S. Sahay, C.P. Malhotra, and A.M. Kolkhede, Accelerated Grain Growth Behaviour During Cyclic Annealing, *Acta Mater.*, 2003, **51**, p 339–346
10. J.D. Verhoeven, The Role of the Divorced Eutectoid Transformation in the Spheroidization of 52100 Steel, *Metall. Mater. Trans. A*, 2000, **31A**, p 2431–2438
11. J.D. Verhoeven and E.D. Gibson, The Divorced Eutectoid Transformation in Steel, *Metall. Mater. Trans. A*, 1998, **29A**, p 1181–1189
12. G.R. Speich and A. Szirmae, Formation of Austenite from Ferrite and Ferrite-Carbide Aggregates, *Trans. Metall. Soc. AIME*, 1969, **245**, p 1063–1074
13. R. Kumar, *Physical Metallurgy of Iron and Steel*, Asia Publishing House, Bombay, 1968, p 92–93